

ACCEPTED VERSION

Carla M. Zammit, Florian Weiland, Joël Brugger, Benjamin Wade, Lyron Juan Winderbaum, Dietrich H. Nies, Gordon Southam, Peter Hoffmann and Frank Reith

Proteomic responses to gold(III)-toxicity in the bacterium *Cupriavidus metallidurans* CH34

Metallomics, 2016; 8(11):1204-1216

This journal is © The Royal Society of Chemistry 2016

Published at: <http://dx.doi.org/10.1039/c6mt00142d>

PERMISSIONS

<http://www.rsc.org/journals-books-databases/journal-authors-reviewers/licences-copyright-permissions/#deposition-sharing>

Deposition and sharing rights

When the author accepts the licence to publish for a journal article, he/she retains certain rights concerning the deposition of the whole article. This table summarises how you may distribute the accepted manuscript and version of record of your article.

Sharing rights	Accepted manuscript	Version of record
Share with individuals on request, for personal use	✓	✓
Use for teaching or training materials	✓	✓
Use in submissions of grant applications, or academic requirements such as theses or dissertations	✓	✓
Share with a closed group of research collaborators, for example via an intranet or privately via a scholarly communication network	✓	✓
Share publicly via a scholarly communication network that has signed up to STM sharing principles	⌚	✗
Share publicly via a personal website, institutional repository or other not-for-profit repository	⌚	✗
Share publicly via a scholarly communication network that has not signed up to STM sharing principles	✗	✗

⌚ Accepted manuscripts may be distributed via repositories after an embargo period of 12 months

19 October 2017

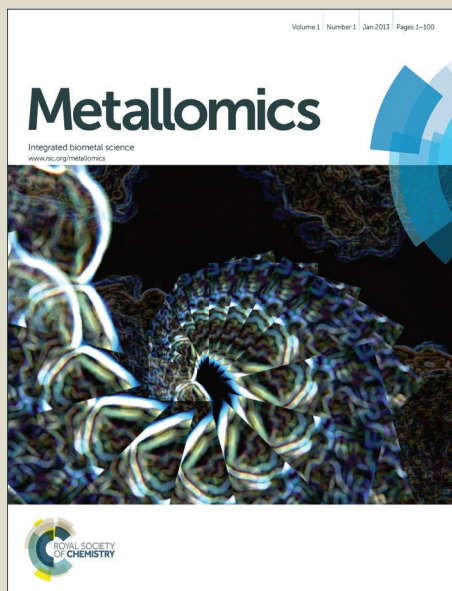
<http://hdl.handle.net/2440/102854>

Metallomics

Accepted Manuscript



This article can be cited before page numbers have been issued, to do this please use: C. M. Zammit, F. Weiland, J. Brugger, B. Wade, L. J. Winderbaum, D. H. Nies, G. Southam, P. Hoffmann and F. Reith, *Metallomics*, 2016, DOI: 10.1039/C6MT00142D.



This is an *Accepted Manuscript*, which has been through the Royal Society of Chemistry peer review process and has been accepted for publication.

Accepted Manuscripts are published online shortly after acceptance, before technical editing, formatting and proof reading. Using this free service, authors can make their results available to the community, in citable form, before we publish the edited article. We will replace this *Accepted Manuscript* with the edited and formatted *Advance Article* as soon as it is available.

You can find more information about *Accepted Manuscripts* in the [Information for Authors](#).

Please note that technical editing may introduce minor changes to the text and/or graphics, which may alter content. The journal's standard [Terms & Conditions](#) and the [Ethical guidelines](#) still apply. In no event shall the Royal Society of Chemistry be held responsible for any errors or omissions in this *Accepted Manuscript* or any consequences arising from the use of any information it contains.

Confidential Information: Revised (2) manuscript re-submitted to Metallogenics

Proteomic responses to gold(III)-toxicity in the bacterium *Cupriavidus metallidurans* CH34

Carla M. Zammit¹, Florian Weiland^{2,3}, Joël Brugger⁴, Benjamin Wade⁵, Lyron Juan Winderbaum², Dietrich H. Nies⁶, Gordon Southam¹, Peter Hoffmann^{2,3} and Frank Reith^{7,8*}

¹ University of Queensland, Earth Sciences; St Lucia, Brisbane, Queensland 4072, Australia

² Adelaide Proteomics Centre, School of Molecular and Biomedical Science, University of Adelaide; Adelaide 5005, Australia

³ Institute for Photonics and Advanced Sensing, University of Adelaide; Adelaide 5005, Australia

⁴ Monash University, Earth, Atmosphere, and the Environment; Clayton, Victoria 3800, Australia

⁵ The University of Adelaide, Centre for Advanced Microscopy and Microanalysis; South Australia 5005, Australia

⁶ Institut für Mikrobiologie, Martin-Luther-Universität Halle; 06120 Halle, Germany

⁷ The University of Adelaide, School of Biological Sciences, The Sprigg Geobiology Centre, Adelaide, South Australia 5005, Australia

⁸ CSIRO Land and Water, Environmental Contaminant Mitigation and Technologies, PMB2, Glen Osmond, South Australia 5064, Australia

* Corresponding Author: Frank Reith, E: frank.reith@csiro.au, T: +61 8 8303 8469, Fax: +61 8 8303 8550

1 Running Title: Gold(III)-toxicity in *Cupriavidus metallidurans* CH34

3 Abbreviations:

4 BN-PAGE: blue-native polyacrylamide gel electrophoresis

5 IPS: Internal pooled standard

6 LA-ICP-MS: Laser ablation inductively coupled plasma mass spectrometry

7 PCA: Principal component analysis

8 PHA: Poly-hydroxyalkanoates

9 PHB: Poly-hydroxybutyrate

10 rpm: revolutions per minute

11 RT: room-temperature

12 SD: standard deviation

Abstract

The metal-resistant β -Proteobacterium *Cupriavidus metallidurans* drives gold (Au) biomineralisation and the (trans)formation of Au nuggets largely via unknown biochemical processes, ultimately leading to the reductive precipitation of mobile, toxic Au(I/III)-complexes. In this study proteomic responses of *C. metallidurans* CH34 to mobile, toxic Au(III)-chloride are investigated. Cells were grown in the presence of 10 and 50 μ M Au(III)-chloride, 50 μ M Cu(II)-chloride and without additional metals. Differentially expressed proteins were detected by difference gel electrophoresis and identified by liquid chromatography coupled mass spectrometry. Proteins that were more abundant in the presence of Au(III)-chloride are involved in a range of important cellular functions, e.g., metabolic activities, transcriptional regulation, efflux and metal transport. To identify Au-binding proteins, protein extracts were separated by native 2D gel electrophoresis and Au in protein spots was detected by laser absorption inductively coupled plasma mass spectrometry. A chaperon protein commonly understood to bind copper (Cu), CupC, was identified and shown to bind Au. This indicates that it forms part of a multi-metal detoxification system and suggests that similar/shared detoxification pathways for Au and Cu exist. Overall, this means that *C. metallidurans* CH34 is able to mollify the toxic effects of cytoplasmic Au(III) by sequestering this Au-species. This effect may in the future be used to develop CupC-based biosensing capabilities for the in-field detection of Au in exploration samples.

Significance to Metallomics

The bacterium *Cupriavidus metallidurans* CH34 is known to survive on the surface of and (trans)form natural gold grains. It reacts to the toxicity induced by mobile gold-complexes using a range of proteomic responses. Specifically, *C. metallidurans* overexpresses the chaperone protein CupC, which binds cytoplasmic gold, forms part of a multi-metal detoxification system to export

1 1 gold, likely using ATPase metal efflux proteins. To support gold detoxification, proteins involved in
2
3
4 2 oxidative stress reduction, energy metabolism and lipid formation are produced.
5
6
7 3
8
9
10
11
12
13
14
15
16
17
18
19
20
21
22
23
24
25
26
27
28
29
30
31
32
33
34
35
36
37
38
39
40
41
42
43
44
45
46
47
48
49
50
51
52
53
54
55
56
57
58
59
60

Metallomics Accepted Manuscript

1. Introduction

The metallophilic β -Proteobacterium *Cupriavidus metallidurans* CH34 was first isolated from a decantation tank at a zinc factory in Belgium.¹ Since then it has been detected in variety of metal-rich environments, e.g., industrial sites around the world as well as the cooling water of the Russian Space Station.^{2,3} *C. metallidurans* has been shown to be highly adaptive to changing environmental conditions, possibly because its genome readily incorporates and expresses foreign genes.⁴ Heavy metal resistance genes have been acquired, re-combined and re-arranged from a range of sources; hence, the genome of *C. metallidurans* CH34 has undergone many alterations, which have allowed it to inhabit a wide range of environments containing high concentrations of heavy metals.^{4,5} It harbours a genetic system with at least 25 *loci* for heavy metal resistance located in two large circular chromosomes and two megaplasmids.^{4,5} Therefore, it has become a model organism to study microbial responses to heavy metals and its extreme tolerance to a range of metals including Ag(I), AsO₃⁻, Au(I), Au(III), Bi(III), Co(II), Cd(II), CrO₄²⁻, Cs(I), Cu(I), Cu(II), HAsO₄²⁻, Hg(II), Ni(II), Pb(II), SeO₃²⁻, SeO₄²⁻, Sr(II), Ti(I) and Zn(II) has been assessed in a range of studies.^{4,5}

Advances in microscopic, micro-analytical and molecular techniques have facilitated an evolution in our understanding of how microorganisms interact with metals in the environment. With regards to Au, the element is no longer thought of as a stable and inert substance under Earth surface conditions. Rather, microorganisms have been shown to play a fundamental role in the solubilisation, transportation and re-concentration of Au in Earth surface environments.^{6,7} Understanding the role *C. metallidurans* plays in the biogeochemical cycling of Au and Au nugget (trans)formation is of particular interest.^{8,9} *C. metallidurans* has been shown to mobilise Au¹⁰ and dominate biofilm communities inhabiting the surfaces of Au grains from several Australian sites.^{9,11} In quartz-sand-packed column experiments, columns inoculated with *C. metallidurans* retained >99

1 wt% of percolating highly toxic Au(I)-thiosulfate (Minimal Inhibitory Concentration (MIC) = 0.5 μ M),
2 in comparison to <30 wt.% retained in sterilised or abiotic controls.¹² Here the formation of
3 intracellular Au nanoparticles and extracellular micro-nuggets was also observed.¹² To survive such
4 close associations with Au, *C. metallidurans* CH34 needs to be able to detoxify Au-complexes.

5 By grouping the treatment of toxic metals into the same transcriptional network, organisms
6 are able to detoxify their environment without energetically expensive metal specific resistance
7 systems.^{13,14} For example, in *C. metallidurans*, cellular uptake of Au(I/III)-complexes co-regulates a
8 range of metal export pathways, especially those for Cu, which may be co-utilised for detoxification
9 and export.¹⁵ However, the interpretation of the molecular mechanisms involved in Au(I/III)-
10 detoxification in *C. metallidurans* is complex and is as yet not fully understood. Earlier studies have
11 shown that the *cupRAC* cluster encoding a regulatory protein (CupR), a heavy metal translocation
12 P-type ATPase (CupA) and a heavy metal chaperone protein (CupC), was strongly up-regulated in
13 Au-complexes amended cells.^{8,16} Modified *C. metallidurans* cells, containing an engineered plasmid
14 carrying the red fluorescent protein (*rfp*) gene under the control of the CupR-upregulated promoter
15 *cupC*, showed specific up-regulation of this *cupR(rev)-PcupA/R(rev)-PcupC-rfp* cluster with Au(III)-
16 complexes but not Cu-ions, when induced with 50 μ M of the metals.¹⁷ This led to the development
17 of a highly-selective fluorescence-based whole-cell biosensor for Au-complexes.¹⁷ In another study
18 addition of Au(III)-complexes to the supernatant of a *C. metallidurans* culture, which had expressed
19 truncated CupC, resulted in the formation of Au nanoparticles; note: truncated CupC contained its
20 metal-binding motif and was fused to secretion carrier Rmet_3428, a homolog of known secretion-
21 carrier OsmY found in *Escherichia coli*.¹⁸ However, the majority of studies investigating the
22 response of *C. metallidurans* to Au(I/III) have relied on transcriptomics.^{8,13,15} Transcriptomics uses
23 the amount of mRNA in a cell as an indicator of cellular function, but mRNA abundance is not
24 necessarily indicative of protein abundance or cellular function. Therefore, it is important to study all
25 levels of molecular expression and activity to gain a complete view of microbial responses to
26

1 environmental changes. There have only been a limited number of studies on proteomic changes
2 that occur within *C. metallidurans*, e.g., studies on the effect of Cu¹⁴, Pb¹⁹ and microgravity²⁰. The
3 study investigating the effect of Pb on the proteome of *C. metallidurans* clearly demonstrated one
4 of the advantages of using proteomic techniques to investigate molecular responses of
5 microorganisms to stress.¹⁹

6 In the current study we describe the proteomic response of *C. metallidurans* CH34 to Au(III)
7 compared to control cells amended with Cu(II) and in media without additional metals. Two Au(III)-
8 concentration, i.e., 10 and 50 µM, were chosen to assess a possible dosage effect of Au. Similar to
9 the study by Tseng *et al.*¹⁷, a Cu²⁺-control concentration equal to the highest Au(III)-concentration
10 was chosen, because a central-aim of this study was to explore for Au-binding proteins with the
11 potential for later use in protein-based biosensors. These need to function specifically to the
12 analyte, i.e., Au(III), even if considerable concentration of a potentially cross-regulating/cross-
13 binding metal, i.e., Cu²⁺, is also present in the solution. To effectively analyse the experiments we
14 used techniques that allowed protein isoforms to be detected and proteins to remain intact during
15 separation. As proteins remained intact during separation, spatially resolved laser absorption
16 inductively coupled plasma mass spectrometry (LA-ICP-MS) was used to detect any proteins that
17 directly bind Au.

2. Materials and methods

2.1. Experimental design and statistical procedures

18 Four biological replicates in each of four experimental groups: 10 µM Au(III) stress, 50 µM Au(III)
19 stress, 50 µM Cu(II) stress and an unamended control, producing a total of 16 samples that were
20 analysed by Differential-in-Gel-Electrophoresis (DIGE). The number of biological replicates per
21 group was chosen based on the decision to include a balanced dye-swap design where two

1 biological replicates in each group were labelled with Cy3 and the remaining two with Cy5. After
2 image analysis using DeCyder 7.0 (GE Healthcare, Little Chalfont, United Kingdom), the spot
3 volume data was exported using the DeCyder 7.0 XML toolbox (GE Healthcare) and the individual
4 spot volume data was standardised by the corresponding spot volume of the internal pooled
5 standard (IPS) channel.²¹ The resulting data was log-2 transformed to produce a normal
6 distribution of the standardised spot volumes. For statistical testing, a two-tailed Student's t-test
7 was applied, with a level of significance $\alpha = 0.05$. A t-test was chosen as the interpretation of the
8 resulting p-value is straight forward, being the probability of measuring an extreme distribution of
9 the data points under the assumption of the null hypothesis ($H_0: \mu_1 = \mu_2$). The p-value is used as
10 evidence of two measured distributions not having equal means, which is interpreted as the
11 difference in protein expression between the two tested groups. The false discovery rate was
12 estimated using q-values. False discovery rate can be interpreted as the proportion of proteins
13 exhibiting a p-value below the significance level expected to be type-I errors (Table 1). Assessment
14 of protein expression change was undertaken by calculating the distance in multiples of standard
15 deviations (SD) of each group of measured spot volumes, with 3 SD being set as the cut-off. These
16 protein spots were assigned as the class of primary interest. Principal component analysis (PCA)
17 was used to visualise these high-dimensional data by projecting them into a lower dimensional
18 subspace while preserving the maximum possible amount of variance, and a biplot was used to
19 interpret these principle components in terms of the original variables – *i.e.*, the protein spots with
20 the highest loadings in the respective principal component, contributing the most to these
21 differences.

2.2. Microbial strains and growth conditions

1 1 *C. metallidurans* CH34 was obtained from the Deutsche Sammlung von Mikroorganismen und
2 Zellkulturen GmbH and grown in Tris-buffered mineral salts medium¹ containing 2 g L⁻¹ sodium
3 gluconate at 30°C with shaking at 120 revolutions per minute (rpm). *C. metallidurans* CH34 was
4 initially grown on solid media and a single colony was picked and grown in liquid media, until the
5 exponential growth phase (OD₆₀₀ 0.55 ± 0.05). In 150 mL Erlenmeyer flasks, 10 µL of culture was
6 added to 40 mL of fresh medium and grown to the beginning of the exponential phase (OD₆₀₀ 0.15
7 ± 0.05). At this stage each set of quadruplicate cultures had either 10 µM of Au(III), 50 µM of Au(III)
8 (in the form of AuCl₄) or 50 µM of Cu(II) (in the form of CuCl₂) added. Au(III) was chosen for this
9 study as this form has been shown to be more toxic than Au(I) to *C. metallidurans* CH34 cells.^{8,15}
10 Another quadruplicate set of cultures had no additional metals added, serving as a control. Cultures
11 were left to grow until the end of the exponential phase (OD₆₀₀ 0.55 ± 0.05) and the cells were
12 harvested by centrifugation at 10,000 rpm for 10 min at 4°C. Cells were then washed three times
13 with PBS (137 mM NaCl, 2.7 mM KCl, 10 mM Na₂HPO₄, 2 mM KH₂PO₄) and stored at -80°C. An
14 independent set of biological triplicate cultures was grown under the same conditions as described
15 above for analysis by native 2D gel electrophoresis.

2.3. Protein extraction and purification

18 Washed cells were suspended in 250 µL of Isoelectric Focussing (IEF) sample buffer (7 M urea
19 (Merck, Darmstadt, Germany), 2 M thiourea (GE Healthcare), 30 mM Tris (Merck), 4 % CHAPS
20 (Roche Diagnostics, Basel, Switzerland), 1 % protease inhibitor cocktail (Sigma-Aldrich, St. Louis,
21 Missouri, USA), 1.1 % Pefabloc[®] SC (PSC) protector reagent (Roche Diagnostics), pH 8.5). Cells
22 were lysed using an ultrasonic probe (B-30, Branson Danbury, Connecticut, USA); with 30 pulses
23 of sonication (40 % duty cycle), subsequently cooled in ice water for two min, and sonicated for
24 another 30 pulses. Samples were then centrifuged at 20,000 x *g* at 15°C for 60 min and the

1 supernatant was collected and stored at -80°C . The concentration of protein was determined using
2 the EZQ[®] protein quantification assay (Life Technologies, Carlsbad, California, USA) against an
3 ovalbumin standard curve according to the manufacturer's protocol.

2.4. Differential in Gel Electrophoresis (DIGE)

2.4.1. Protein labelling

4 Three $200\text{ pM } \mu\text{L}^{-1}$ solutions of three CyDyes (Cy2, Cy3 and Cy5; GE Healthcare) in anhydrous
5 dimethylformamide were made and stored under Ar in 1 mL aliquots at -80°C . For protein labelling,
6 100 μg of protein from each sample was added to 1 μL of either the Cy3 or Cy5 labelling solutions.
7 IPS was made consisting of 50 μg of protein pooled from each sample and this was labelled with
8 Cy2. Labelling solutions were incubated in the dark at room temperature (RT) for 30 min, upon
9 which the labelling reaction was stopped with the addition of 1 μL of 1 M lysine and incubated in the
10 dark at RT for 10 min. After labelling, 1,4-dithiothreitol (DTT, Roche Diagnostics; 0.1 g dissolved in
11 17 μL H_2O) was added to the solution to a volume of 2 % (v/v) and incubated on ice for 60 min in
12 the dark, then Pharmalyte 3-10 (GE Healthcare) was then added to a volume of 2 % (v/v) and
13 samples were stored at -80°C .

2.4.2. Isoelectric focusing (IEF)

14 Eight IPG strips spanning a 240 mm non-linear pH 3 - 11 range (GE Healthcare) were rehydrated
15 overnight at RT in 450 μL rehydration buffer (6 M urea, 2 M thiourea, 1% CHAPS, 0.5% pH 3 - 11
16 NL carrier ampholytes (GE Healthcare) and 200 mM 2,2'-dithiodiethanol (Sigma-Aldrich). Samples
17 were applied by anodal cup loading. IEF was performed in the dark on an IPGphor II (GE
18 Healthcare) at 20°C using a six step program with the current limited to 50 μA per strip; step one:

1 150 V for 1 h; step two: 300 V for 1 h; step three: 600 V for 2.5 h; step four: 600-8000 V gradient
2 over 1.5 h; step five: 8000 V for 27 kWh.

3 2.4.3. SDS-PAGE

4 Following IEF, strips were equilibrated for 15 min in a proprietary equilibration buffer (Serva
5 Electrophoresis GmbH, Heidelberg, Germany) containing 6M urea and 10 mg mL⁻¹ DTT (Roche
6 Diagnostics). After equilibration, the solution was removed and exchanged with equilibration buffer
7 containing 40 mg mL⁻¹ iodoacetamide (GE Healthcare) instead of DTT. Separation in the second
8 dimension was carried out using 18 x 25 cm² 2D Gel DALT NF flatbed pre-cast polyacrylamide gels
9 (T=12.5%; Serva). Electrophoresis was performed at 7 mA per gel for 1 h, 13 mA per gel for 1 h,
10 then the IPG strip was removed and electrophoresis continued at 40 mA per gel for 3 h and 50 min.

11 2.4.4. Image analysis

12 Gels were scanned using an Ettan DIGE Imager (GE Healthcare) at 100 μm resolution, with the
13 following exposure times; Cy2: 2.50 s; Cy3: 0.45 s; and, Cy5: 0.50 s. ImageQuantTL (GE
14 Healthcare) software was used to orientate gel images and subsequent image analysis was carried
15 out using DeCyder 2D software version 7 (GE Healthcare). The spot detection algorithm was set to
16 an estimate of 5,000 spots. Detected spots were excluded if they exhibited a slope >1.1, an area <
17 300, a volume < 30,000, a peak height < 80 or > 65,534 (to exclude saturated signals). Normalised
18 spot volumes were exported using XML toolbox sub-program of DeCyder 7.0. Data was
19 standardised by the spot volume of the corresponding spot in the Cy2 (IPS) channel. Standardised
20 data was log-2 transformed and statistical significance was tested using a two-tailed Student's t-
21 tests, with significance level $\alpha = 0.05$. PCA and biplot was conducted on the standardised, log-2
22 transformed data using R. Post-hoc power calculation was performed using Piface (v1.64)²² and
23 resulted that a fold-change of 1.7 or 1.6 (as applicable, Table 1) was detected with a probability of
24
25
26
27
28
29
30
31
32
33
34
35
36
37
38
39
40
41
42
43
44
45
46
47
48
49
50
51
52
53
54
55
56
57
58
59
60

1 80 %. The false discovery rate at the significance level was determined using q-values (Table 1) as
2 described in Penno *et al.*²³ Proteins were fixed into the gel using 40 % (v/v) ethanol, 10% (v/v)
3 acetic acid overnight at RT and visualised using Coomassie Brilliant Blue G250. Spots from DIGE
4 gels analysed by mass spectrometry were picked using an Ettan Spot Picker (GE Healthcare). All
5 image files, exported DeCyder analysis file and picking lists can be downloaded from
6 ProteomeXchange PXD005034.

2.5. Native two dimensional-polyacrylamide gel electrophoresis

7
8 Three hundred µg of protein extracts from each of the three biological replicates from the three
9 conditions (Control, 50 µM Cu(III) and 50 µM Au(III)) were separated using native IEF in 11cm IPG
10 pH 3-10NL (Bio-Rad, Hercules, California, USA) in combination with blue native-polyacrylamide gel
11 electrophoresis (BN-PAGE) according to the protocol outlined in.²⁴ Potential protein complexes
12 were visualised using Ag staining.²⁵ Eleven protein spots, which were only visible in all three
13 replicates from cells grown with 50 µM Au(III) (as in comparison with all replicates of the two other
14 conditions), were chosen for further identification by MS.

2.6. Liquid Chromatography-Mass Spectrometry (LC-MS)

15
16 All samples were analysed by either Orbitrap (Thermo-Fisher, Waltham, MA, USA) or amaZon 3D
17 iontrap (Bruker Daltonics, Bremen, Germany) MS. Coomassie-stained spots were destained using
18 30 % (v/v) acetonitrile (Merck) until they appeared blank, in case of silver-stained spots, proteins
19 were destained using rapid fixer (Agfa-Gevaert, Mortsel, Belgium) before reduction and alkylation.²⁶
20 Proteins were digested overnight at 37°C using 100 ng sequencing grade Trypsin (Promega,
21 Madison, USA). For Orbitrap analysis, peptides were separated on a nano-flow Ultimate 3000
22
23
24
25
26
27
28
29
30
31
32
33
34
35
36
37
38
39
40
41
42
43
44
45
46
47
48
49
50
51
52
53
54
55
56
57
58
59
60

1 HPLC system (Dionex, Sunnyvale, USA). Peptides were loaded onto a Acclaim PepMap 100 C18
2 column (3 μm particle size, 75 μM inner diameter, 2 cm length, Thermo-Fischer) and desalted for 5
3 min in buffer A (2 % (v/v) acetonitrile, 0.1 % formic acid) and 5 $\mu\text{L min}^{-1}$ flow rate. Peptides were
4 using a two buffer system (buffer A and buffer B (80 % (v/v) acetonitrile, 0.1 % (v/v) formic acid))
5 separated on a Acclaim PepMap RSLC C18 column (2 μM particle size, 75 μM inner diameter, 15
6 cm length, Thermo-Fischer) using a linear gradient from 5 % buffer B to 45 % buffer B over 29 min,
7 followed by a 90 % buffer B wash for 13 min and column equilibration in 5 % buffer B for 18 min at
8 a flow rate of 300 nL min^{-1} . Column oven temperature was set to 60°C. Peptides were injected in to
9 the Orbitrap via a nano spray ESI source. Orbitrap was set to Nth order double play mode in
10 positive ion mode, scanning between 300-2000 m/z with a set resolution of 60,000. The top 6
11 intense m/z features were subjected to CID MS/MS (minimum signal intensity: 5,000, isolation
12 width: 3.00, normalised collision energy: 35.0). Samples analysed by the amaZon 3D iontrap were
13 separated on an Agilent 1100 nano-flow HPLC (Agilent, Santa Clara, USA). Desalting of peptide
14 mixture was carried out by loading onto a Acclaim PepMap 100 column (same specifications as
15 above) and washing with 100 % buffer C (0.1 % (v/v) formic acid) for 4 min at 5 $\mu\text{L min}^{-1}$. Peptides
16 were separated on a Acclaim PepMap RSLC C18 column (same specifications as above) using a
17 two buffer system (buffer C and buffer D (90 % (v/v) acetonitrile, 0.1 % formic acid) in a linear
18 gradient from 5 % to 45 % buffer B over 17 min, followed by a 5 min 95% buffer B and a 3 minute
19 equilibration step with 5 % buffer B. AmaZon Iontrap was set for enhanced resolution scan in
20 positive mode between 300-200 m/z and 3 most ionisable features were chosen for CID
21 fragmentation.

22 Orbitrap and amazon Iontrap raw data was converted to mzXML format using Proteowizard
23 software²⁷ and submitted to Comet version 2016.2²⁸. Processed data was searched against NCBI
24 database of human, porcine trypsin and *C. metallidurans* CH34 (28,243 sequences), downloaded
25
26
27
28
29
30

1 on 25/07/2016. Search parameters applied for Comet search were: precursor mass tolerance of
2 either 20 ppm (Orbitrap) or 0.4 Da (ion-trap MS), fragment bin size was set to 1.005, trypsin was
3 set as protease (no cleavage after proline), a maximum of two missed cleavages was allowed,
4 while fixed modification was set as carbamidomethyl (C) and variable modification as oxidation (M).
5 Proteins were considered identified if two peptides with an expectation below 0.05 using the comet
6 scoring algorithm were detected. In case of spots picked from DIGE gels, if more than one protein
7 was identified per cut-out gel spot, the protein with the largest number expressed as product of
8 unique sequences and protein coverage was chosen over the other proteins. In case these number
9 was similar among the identified proteins, all these proteins are reported. As Comet could not
10 provide details to the matched fragment ions, a MASCOT (version 2.3.01, Matrix Sciences, UK)
11 search of the MS data of Spot 9 and the designated protein spot corresponding to the Au signal on
12 the native 2D gels was performed for easy visualisation (see Supplement S1). For this, 3D ion trap
13 raw data was converted to mgf by Proteowizard software. Parameter deviating from the comet
14 search, using MASCOT were as follows: 0.4 Da fragment mass tolerance, re-scoring using
15 percolator. All mzXML & pep.xml files, exported MASCOT xml and processed results files and
16 Comet search parameters can be downloaded from ProteomeXchange PXD004199.

2.7. Native 2D Western-blot

17 Gel for n2D-PAGE was cast and electrophoresis was performed according to the protocol
18 described above. Three hundred μg protein extract from *C. metallidurans CH34* cells grown in 50
19 μM Au(III) was separated by native IEF. Before BN-PAGE as second dimension, 100 μg protein
20 extract of *C. metallidurans CH34* cells grown in 50 μM Au(III) was mixed with 1.8 μL 5 % (w/v)
21 Coomassie G-250 (Sigma-Aldrich) in H_2O and filled up to a volume of 10 μL with Equilibration
22 Buffer.²⁴ This mixture was pipetted onto a filter paper (3 mm CHR, Whatman, Maidstone, United
23
24
25
26
27
28
29
30
31
32
33
34
35
36
37
38
39
40
41
42
43
44
45
46
47
48
49
50
51
52
53
54
55
56
57
58
59
60

1 Kingdom) and placed onto the upper edge of the gel next to the equilibrated IPG strip, serving as
2 primary marker lane for subsequent LA-ICP-MS. After BN-PAGE, proteins were transferred by a
3 Criterion wet-blotting system (Bio-rad) to a PVDF membrane (Merck) using the buffer system
4 described in Wittig *et al.*²⁹ with the following settings: 400 mA for 2 h at RT, limited to 70 V.

2.8. Laser Ablation Inductively Coupled Plasma Mass Spectrometry (LA-ICP-MS)

5 The PVDF membranes from the native 2D WB was backed onto quartz slides. LA-ICP-MS mapping
6 was conducted using a Resonetics M-50-LR 193 nm Excimer laser coupled to an Agilent 7700cx
7 Quadrupole ICP-MS housed at Adelaide Microscopy (Table S1). Ablation was carried out in a two-
8 volume ablation cell designed by Laurin Technic Pty using UHP He (0.7 L min⁻¹) as a carrier gas.
9 Immediately upon exiting the cell, the aerosol cell was mixed with Ar (0.93 L min⁻¹) and passed into
10 the torch. The ICP-MS was optimised to maximise sensitivity on isotopes of the mass range of
11 interest, while keeping production of molecular oxide species (*i.e.*, ²³²Th¹⁶O/²³²Th) and doubly
12 charged ion species (*i.e.*, ¹⁴⁰Ce²⁺/¹⁴⁰Ce⁺) as low as possible, and usually <0.2 %.

13 Analysis was performed by ablating sets of parallel line rasters in a grid across the samples.

14 A beam size of 300 μm and a scan speed of 150 μm s⁻¹ were chosen which resulted in the desired
15 sensitivity of elements of interest, and adequate spatial resolution for the study. A laser repetition of
16 10 Hz was used at a constant energy output of 80 mJ, resulting in an energy density of ~4 J cm⁻² at
17 the target. Using these beam conditions depth of ablation during mapping was around 10 μm. A set
18 of 8 elements (¹³C, ²⁹Si, ³¹P, ³⁴S, ⁶⁰Ni, ⁶⁵Cu, ⁶⁶Zn, ¹⁹⁷Au) were analysed with dwell time for all
19 masses set to 0.003 s, resulting in a total sweep time was ~0.07 s. A 30 s background acquisition
20 was acquired at the start of every raster, and to allow for cell wash-out, gas stabilisation, and
21 computing processing, a delay of 15 s was used after each line. Identical rasters were done on
22 NIST SRM 610 at the start and end of a mapping run. Upon detection of Au in the primary marker
23
24
25
26
27
28
29
30
31
32
33
34
35
36
37
38
39
40
41
42
43
44
45
46
47
48
49
50
51
52
53
54
55
56
57
58
59
60

1 lane, the laser ablation was continued in perpendicular direction to pin-point the gold signal to a
2 specific protein signal in the n2D-PAGE part of the blot. After LA-ICP-MS the blot was stained using
3 Coomassie R250. The resulting protein pattern and the locus of Au was compared to silvers
4 stained native 2D gels and the corresponding spot was identified by mass spectrometry as
5 described above.

2.9. Structural and interaction analyses of proteins

A search of the NCBI database (blast.st-va.ncbi.nlm.nih.gov/Blast.cgi)³⁰ returned Cu chaperon proteins that only consisted of amino acids 68-133, therefore only these amino acids were used for further analysis. A model of this protein was made using the SWISS-MODEL program (swissmodel.expasy.org/)³¹ with the *C. metallidurans* CH34 genome (NCBI Accession: PRJDB279). The following templates were selected from a search of the Protein DataBank (pdb.org)³² and used to construct a model: 2rml.1.A, a copper transporting P-type ATPase CopC; 2rog.1.A and 2roe.1.A, both heavy metal binding proteins.³³⁻³⁶ STRING (Search Tool for Retrieval of Interacting Genes/Proteins; <http://string-db.org>) was used to visualise predicted protein-protein interactions for the Au-binding protein detected.³⁷

3. Results and discussion

3.1. DIGE-analyses of differentially expressed proteins

In total 2,196 protein spots were detected by DeCyder (Fig. 1). Of the 1,597 proteins spots detected in at least two samples, of each of the four experimental groups, 59 exhibited a very stringent (p -value < 0.001) expression pattern of up-regulation in both Au groups compared to both Cu and unamended control groups (Table S2). Principle component analysis of the DIGE data

1 (using the 864 protein spots detected in all 16 samples) showed that the first principle component
2 produces a clear separation of Au-amended cells to unamended cells and Cu-controls, with the fifth
3 principle component separating the 10 μM from the 50 μM Au group (Fig. 2 A ,B). This
4 demonstrates a specific proteomic response of *C. metallidurans* to increasing Au(III)-stress under
5 these conditions.

6 We were most interested in proteins that exhibited up-regulation in both Au concentrations in
7 comparison to both controls; 183 protein spots exhibited this pattern. Of these 183 proteins, 60
8 were also differentially abundant between the Cu-amended experiment and the unamended
9 control, leaving 123 spots that were uniquely more abundant in both Au groups with no statistically
10 significant change in expression between Cu and the control (p -value >0.05 ; Fig. 3A). Forty two of
11 the 123 protein spots in greater abundance exhibited a very stringent expression pattern and were
12 three times the standard deviation from the mean (Table S2). Twenty-nine of these proteins,
13 showing the highest degree of differential expression were successfully identified by MS (Table 2A,
14 Table S3).

15 These proteins are involved in a range of metabolic activities, transcriptional regulators,
16 efflux proteins, and transporters (Fig. 3B; Table 2, Table S3). Specifically, a predicted DNA-binding
17 transcriptional repressor was identified (spot 1237; Table 2). The sequence of this DeoR family
18 protein contains a region that has been shown to regulate carbohydrate transport and metabolism
19 in *Corynebacterium glutamicum* ATCC 13032.³⁸ A protein disaggregation chaperon was identified
20 (spot 259), this protein disaggregates miss folded and aggregated proteins.³⁹ DNA gyrase subunit
21 B was identified from spot 256, this protein contains a metal (Mg^{2+}) binding site. Other notable
22 proteins were identified such as a DNA-binding transcriptional repressor (spot 1237). Five proteins
23 spots demonstrated a dosage response between 50 μM Au and 10 μM Au (spot 586, 609, 863, 977
24 and 1681; Fig. 3A; Table S2). The identified metabolic proteins provide an indication that cells are

1 1 adjusting to increased stress, they are: i) the ABC-type sugar periplasmic transporter involved in
2 2 carbohydrate transport and metabolism, ii) glyceraldehyde-3-phosphate dehydrogenase involved in
3 3 a range of metabolic functions, iii) acetyl-CoA acetyltransferase, and iv) sn-glycerol-3-phosphate
4 4 dehydrogenase (FAD/NAD(P)-binding protein) involved in linking carbohydrate and lipid
5 5 metabolism (Table 2, Table S3).⁴⁰⁻⁴² The greater abundance of metabolism proteins (Fig. 3B)
6 6 suggests that cells are increasing metabolic rates and energy production so that biochemical
7 7 mechanisms to deal with elevated Au-stress can be activated. Oxidative stress from Au(III)-
8 8 complexes causes cell membrane damage, hence the overexpression of sn-glycerol-3-phosphate
9 9 dehydrogenase suggests that *C. metallidurans* CH34 is repairing oxidative damage to the cell
10 10 membrane.⁴³

3.2. Native 2D electrophoretic analysis of differentially expressed protein complexes

11 11 Blue native 2D electrophoresis was performed to explore the effect of Au(III)-stress on
12 12 *C. metallidurans* CH34 protein complexes and protein-protein interactions (PPI), compared to Cu-
13 13 and unamended controls. Eleven protein spots were detected, which were only present when
14 14 *C. metallidurans* CH34 was grown in the presence of Au(III)-chloride (Fig. 4). These protein
15 15 complexes and PPI were scattered over a pI range from 3-10 and exhibit molecular weights up to
16 16 approximately 800 kDa. Excised proteins were identified using MS (Table 3, Table S4). Proteins
17 17 involved in cell membrane signalling, as identified using both protein separation methods, indicate
18 18 that cells are undergoing stress (Table 2 and 3). Spot 1 was identified as a signal peptide protein
19 19 that contains conserved regions of a periplasmic or secreted lipoprotein. Other proteins known to
20 20 be involved in managing oxidative stress were also identified, these include a lipid hydro-peroxide
21 21 peroxidase (Spot 5) capable of catalysing oxidation reactions and protein from the OhrB, OsmC
22 22 family (Spots 9, 10 and 11). Spot 6 was identified as alkyl hydro-peroxidase, this protein catalyses
23 23
24 24
25 25
26 26
27 27
28 28
29 29
30 30
31 31
32 32
33 33
34 34
35 35
36 36
37 37
38 38
39 39
40 40
41 41
42 42
43 43
44 44
45 45
46 46
47 47
48 48
49 49
50 50
51 51
52 52
53 53
54 54
55 55
56 56
57 57
58 58
59 59
60 60

1 the reduction of peroxides, which are likely formed when Au-complexes reach the cytoplasm.⁸ This
2 shows that Au(III) induces strong oxidative stress in the cells and confirms the results of earlier
3 transcriptomic studies, in which the genes for these proteins were also strongly expressed.⁸

4 (R)-3-hydroxybutyryl-CoA dehydrogenase PhaB (Spot 3) was also identified. (R)-3-
5 hydroxybutyryl-CoA dehydrogenase is an enzyme that catalyses the NADPH-dependent reduction
6 of acetoacetyl-CoA, an intermediate of polyhydroxyalkanoates (PHA) synthetic pathways.⁴⁴ Poly-
7 hydroxybutyrate (PHB) is the best known PHA and has been implicated in the intracellular
8 storage/resistance to heavy metals.⁴⁵ In the closely related β -Proteobacterium *Burkholderia*
9 *cepacia*, polyhydroxybutyrate (PHB) production occurs when cells are grown in the presence of
10 0.5–5mM Au(I)-thiolates, the polyhydroxybutyrate granules are associated with the storage and
11 passivation of these Au-complexes.⁴⁶ Another hypothetical protein was identified (spot 4), however
12 the function of this protein is unknown. Other proteins identified were largely associated with
13 energy metabolism. Spots 2 was identified as malate synthase. Malate synthase works together
14 with isocitrate lyase in the glyoxylate cycle to bypass two oxidative steps of Krebs cycle and permit
15 C incorporation from acetate or fatty acids in many microorganisms.⁴⁷ Malate dehydrogenase
16 (Spots 5, 5a) is an enzyme that reversibly catalyses the oxidation of malate to oxaloacetate using
17 the reduction of NAD⁺ to NADH.⁴⁸ This reaction is part of many metabolic pathways, including the
18 citric acid cycle.⁴⁸ This strong up-regulation of metabolic genes involved in energy generation,
19 which was also observed in DIGE separation (this study) and in an earlier transcriptomic study,⁸
20 suggests that cells increase metabolic energy generation to enable the production of stress-coping
21 proteins.

3.3. Identification of Au-binding proteins

1 La-ICP-MS on native 2D Western Blot was used to identify Au-binding proteins and yielded one
2 spot containing a high counts for Au, while the count rate for other elements, especially the tested
3 metals, remained at background levels (Fig. 5). Four proteins were identified by MS at the spot
4 where Au was detected: i) 3-demethylubiquinone-9 3-methyltransferase (accession number:
5 93357244), ii) a putative glyoxalase/blemycin resistance protein (499835771), iii) a hypothetical
6 protein (657067637), and iv) a Cu chaperone CupC (93356308) (Table 4, Table S5). The Cu
7 chaperone protein, CupC, was used for further analysis, as this was the only protein to contain a
8 metal binding domain that could be responsible for binding Au-complexes.¹⁸

9 A model of the Cu chaperon protein was constructed based on two related Cu-binding
10 proteins: a 'multispecies' copper chaperone, heavy metal binding (modular protein) of an organism
11 described solely as *Cupriavidus* (WP_00864966) which had a 100% homology between amino
12 acids 68-133 with the Cu chaperon protein identified in this study, and a copper chaperone from
13 *Cupriavidus* sp. BIS7 (WP_019451883); the resulting protein model is shown in Fig. 6.
14 Computational simulation analysis of the protein model recognised eight ligand hits: C₂H₃O₂⁻,
15 Ca(II), Cl⁻, Cu(II), Cu(I), C₃H₈O₃, Na and Zn(II), while Au(I) and Au(III) ligands were not predicted to
16 bind to the protein model. However, the presence of Cu(I)-binding sites demonstrates that the
17 protein CupC contains metal-binding sites that are suitable for Au(I)-binding, due to chemical
18 similarity Au complexes are predicted to bind to Cu-binding sites.⁴ In addition, a study by Ouyang *et*
19 *al.*,¹⁸ showed that Au nanoparticles were formed in the presence of truncated CupC fused to the
20 secretion carrier Rmet_3428, suggesting the binding of Au to a metal-binding motif in CupC.
21 Overall, this highlights the limitations of computer-based protein modelling, which relies on the
22 utilisation of suitable datasets that is not available for the Au-complex studied.

23 An earlier study using transcriptomic approaches had shown a strong up-regulation of the
24 entire metal resistance and efflux operon *cupRAC* (Rmet 3523-3525).⁸ Although the increased
25 transcriptional expression of *cupR* and *cupA* have been shown the resulting proteins were not

1 identified in this study as differentially more abundant or Au-containing in Au amended cells. This
2 may be due to experimental and analytical setup, e.g., very strict criteria were employed to target
3 proteins to be identified by mass spectrometry, which may have excluded them, or masking
4 through co-migrating proteins. Another possibility might that the use of a 3-11 immobilised pH
5 gradient CupAR were not properly resolved and their signals where overlain by co-migrating
6 proteins. While *cupA*, the gene encoding the *C. metallidurans* ortholog of the Cu efflux pump used
7 by *S. enterica* for Au export and detoxification, was strongly expressed, Wiesemann *et al.*¹⁵ have
8 shown that it is likely not involved in the direct Au efflux, and may have another role in Au
9 detoxification.¹⁵ STRING analysis of CupC environment has shown that CupC may interact
10 with/bind to a range metal-transporting ATPases, i.e., CadA, RdxI and CtpA1, which may also be
11 involved in Au-efflux, resistance and biomineralisation (Fig. 6); note setting for STRING analysis
12 allow experimental evidence to be transferred from other organisms.^{49,50} This suggest that CupA
13 may not be Au binding and/or that Au may be transferred to other efflux pumps. Upregulation of
14 *cupR* in *C. metallidurans* suggests that CupR may act as Au-sensing regulator, similar to its
15 homologs GoIS in *Salmonella* and CueR in *E. coli*.^{51,52} In addition, binding of Au-complexes to
16 CupR has been demonstrated by Jian *et al.*,¹⁶ and Tseng *et al.*¹⁷ The affinity of CueR for copper is
17 in the zeptomolar range,⁵³ and that of CupR for Au(I) might be even higher.^{16,17} Therefore, only
18 very few Au-complexes may be required in the cytoplasm for up-regulation of genes by CupR,
19 which appears to lead to a highly elevated production of the CupC. The majority of cytoplasmic Au-
20 complexes is then likely bound by the highly abundant metal-chaperone CupC. This, in combination
21 with using Western-blotting may explain why only highly abundant CupC-Au, but not CupR-Au, was
22 detected using LA-ICP-MS.

4. Conclusions

1 A combination of proteomic and micro-analytical techniques provided a detailed assessment of the
2 proteomic reactions triggered by mobile Au(III)-complexes, which may be employed by *C.*
3 *metallidurans* CH34 to survive on the surface of Au grains. This study shows that Au-complexes
4 reach the cytoplasm. *C. metallidurans* CH34 uses chaperone CupC to bind Au and effect
5 detoxification by export, likely utilising ATPase metal efflux proteins otherwise utilised for a range of
6 metals. To support this detoxification and/or deal with Au-complex toxicity effects, proteins involved
7 in oxidative stress, energy metabolism and lipid formation are more abundant when
8 *C. metallidurans* CH34 was grown in the presence of Au(III). These include sn-glycerol-3-
9 phosphate dehydrogenase, glutathione peroxidase, glutathione S-transferase, lipid hydroperoxide
10 peroxide, the hypothetical protein Rmet_3428 and glyceraldehyde-3-phosphate dehydrogenase.
11 The greater abundance of proteins related to membrane lipids indicates that cell membrane
12 damage is occurring in the presence of metals and *C. metallidurans* CH34 is mitigating this
13 damage by increasing the production of membrane lipids. In addition, proteins like glutathione
14 peroxidase, glutathione S-transferase and lipid hydro-peroxide peroxide help to protect the cell
15 membrane from oxidative stress, which is caused by the accumulation of intracellular Au.

Acknowledgements

The support of the Australian Research Council (LP100200102 and FT150100250 to F.R.), CSIRO
Land and Water, South Australian Museum, The University of Adelaide (UoA), Newmont Pty Ltd.
and Barrick Gold of Australia Ltd., the Environment Institute (UoA), Adelaide Proteomics Centre
and Adelaide Microscopy (UoA). We thank the editor Dr S. Farley for her handling of the
manuscript and the anonymous reviewers for their reviews, which improved the manuscript.

1
2
3
4
5
6
7
8
9
10
11
12
13
14
15
16
17
18
19
20
21
22
23
24
25
26
27
28
29
30
31
32
33
34
35
36
37
38
39
40
41
42
43
44
45
46
47
48
49
50
51
52
53
54
55
56
57
58
59
60

References

1. Mergeay M, Nies D, Schlegel HG, Gerits J, Charles P, Van Gijsegem F. *Alcaligenes eutrophus* CH34 is a facultative chemolithotroph with plasmid-bound resistance to heavy metals. *J. Bacteriol.* 1985; 162, 328-334
2. Mijndonckx K, Provoost A, Ott CM, Venkateswaran K, Mahillon J, Leys N, et al. Characterisation of the survival ability of *Cupriavidus metallidurans* and *Ralstonia pickettii* from space-related environments. *Microb. Ecol.* 2013; 65, 347-360
3. Ott CM, Bruce RJ, Pierson DL. Microbial characterisation of free floating condensate aboard the Mir space station. *Microb. Ecol.* 2004; 47, 133-136
4. Janssen PJ, Van Houdt R, Moors H, Monsieurs P, Morin N, Michaux A, et al. The complete genome sequence of *Cupriavidus metallidurans* strain CH34, a master survivalist in harsh and anthropogenic environments. *PLoS ONE* 2010; 5, e10433
5. Nies DH. The biological chemistry of the transition metal “transportome” of *Cupriavidus metallidurans*. *Metallogenics*, 2016, 8, 481-507.
6. Southam G., Lengke MF, Fairbrother L, Reith F. The biogeochemistry of gold. *Elem.* 2009; 5, 303-307.
7. Rea MA, Zammit CM, Reith F. Bacterial biofilms on gold grains - implications for geomicrobial transformations of gold. *FEMS Microbiol. Ecol.* 2016; 92, fiw082.
8. Reith F, Etschmann B, Grosse C, Moors H, Benotmane MA, Monsieurs P, et al. Mechanisms of gold biomineralization in the bacterium *Cupriavidus metallidurans*. *Proc. Natl. Acad. Sci.* 2009; 106, 17757-17762

- 1 9. Reith F, Fairbrother L, Nolze G, Wilhelmi O, Clode PL, Gregg A, et al. Nanoparticle factories:
2 Biofilms hold the key to gold dispersion and nugget formation. *Geology* 2010; 38, 843-846
3
4 10. Brugger J, Etschmann B, Grosse C, Plumridge C, Kaminski J, Paterson D, et al. Can
5 biological toxicity drive the contrasting behaviour of platinum and gold in surface environments?
6 *Chem. Geol.* 2013; 343, 99-110
7
8 11. Reith F, Rogers SL, McPhail DC, Webb D. Biomineralization of gold: biofilms on
9 bacterioform gold. *Science* 2006; 313, 233-236
10
11 12. Fairbrother L, Etschmann B, Brugger J, Shapter J, Southam G, Reith F. Biomineralization of
12 gold in biofilms of *Cupriavidus metallidurans*. *Environ. Sci. Technol.* 2013; 47, 2628-2635
13
14 13. Monsieurs P, Moors H, Van Houdt R, Janssen PJ, Janssen A, Coninx I, et al. Heavy metal
15 resistance in *Cupriavidus metallidurans* CH34 is governed by an intricate transcriptional network.
16 *Biometals* 2011; 24, 1133-1151
17
18 14. Monchy S, Benotmane MA, Wattiez R, van Aelst S, Auquier V, Borremans B, et al.
19 Transcriptomic and proteomic analyses of the pMOL30-encoded copper resistance in *Cupriavidus*
20 *metallidurans* strain CH34. *Microbiol.* 2006; 152, 1765-1776
21
22 15. Wiesemann N, Mohr J, Grosse C, Herzberg M, Hause G, Reith F, et al. Influence of copper
23 resistance determinants on gold transformation by *Cupriavidus metallidurans* strain CH34. *J.*
24 *Bacteriol.* 2013; 195, 2298-2308
25
26 16. Jian X, Wasinger EC, Lockhard JV, Chen LX, He C. Highly sensitive and selective gold(I)
27 recognition by a metalloregulatory in *Ralstonia metallidurans*. *J. Am. Chem. Soc.* 2009; 131,
28 10869-10871.
29
30
31
32
33
34
35
36
37
38
39
40
41
42
43
44
45
46
47
48
49
50
51
52
53
54
55
56
57
58
59
60

- 1 17. Tseng H, Tsai Y, Yen J, Chen P, Yeh Y. A fluorescence-based microbial sensor for the
2 selective detection of gold. *Chem. Commun.* 2014; 50, 1735-1737.
- 3 18. Ouyang C, Lin Y, Tsi D, Yeh Y. Secretion of metal-binding proteins by a newly discovered
4 OsmY homolog in *Cupriavidus metallidurans* for the biogenic synthesis of metal nanoparticles.
5 *RSC Adv.* 2016; 6, 16798-16801.
- 6 19. Taghavi S, Lesaulnier C, Monchy S, Wattiez R, Mergeay M, van der Lelie D. Lead(II)
7 resistance in *Cupriavidus metallidurans* CH34: interplay between plasmid and chromosomally-
8 located functions. *Antonie van Leeuwenhoek* 2009; 96, 171-182
- 9 20. Leroy B, Rosier C, Erculisse V, Leys N, Mergeay M, Wattiez R. Differential proteomic
10 analysis using isotope-coded protein-labeling strategies: Comparison, improvements and
11 application to simulated microgravity effect on *Cupriavidus metallidurans* CH34. *Proteomics* 2010;
12 10, 2281-2291
- 13 21. Alban A, David SO, Bjorkesten L, Andersson C, Sloge E, Lewis S, et al. A novel
14 experimental design for comparative two-dimensional gel analysis: two-dimensional difference gel
15 electrophoresis incorporating a pooled internal standard. *Proteomics* 2003; 3, 36-44
- 16 22. Lenth RV. Statistical power calculations. *J Ani. Sci.* 2007; 85, E24-29
- 17 23. Penno MA, Klingler-Hoffmann M, Brazzatti JA, Boussioutas A, Putoczki T, Ernst M, et al.
18 2D-DIGE analysis of sera from transgenic mouse models reveals novel candidate protein
19 biomarkers for human gastric cancer. *J. Proteomics* 2012; 77, 40-58.
- 20 24. Weiland F, Zammit CM, Reith F, Hoffmann P. High resolution two-dimensional
21 electrophoresis of native proteins. *Electrophor.* 2014; 35, 1893-1902.

- 1 25. Blum H, Beier H, Gross H. Improved silver staining of plant proteins, RNA and DNA in
2 polyacrylamide gels. *Electrophor.* 1987; 8, 93-99
- 3 26. Shevchenko A, Tomas H, Havlis J, Olsen JV, Mann M. In-gel digestion for mass
4 spectrometric characterization of proteins and proteomes. *Nat. Protoc.* 2006; 1, 2856-2860.
- 5 27. Chambers MC, Maclean B, Burke R, Amodei D, Ruderman DL, Neumann S, et al. A cross-
6 platform toolkit for mass spectrometry and proteomics. *Nat Biotech* 2012; 30, 918-920.
- 7 28. Eng JK, Jahan TA, Hoopmann MR. Comet: an open-source MS/MS sequence database
8 search tool. *Proteomics* 2013; 13, 22-24.
- 9 29. Wittig I, Braun HP, Schagger H. Blue native PAGE. *Nat. Protoc.* 2006; 1, 418-428.
- 10 30. Altschul SF, Madden TL, Schaffer AA, Zhang J, Zhang Z, Miller W, et al. Gapped BLAST
11 and PSI-BLAST: a new generation of protein database search programs. *Nucleic Acids Res.* 1997;
12 25, 3389-3402
- 13 31. Schwede T, Kopp J, Guex N, Peitsch MC. SWISS-MODEL: An automated protein
14 homology-modeling server. *Nucleic Acids Res.* 2003; 31, 3381-3385
- 15 32. Berman HM, Westbrook J, Feng Z, Gilliland G, Bhat TN, Weissig H, Shindyalov IN, Bourne
16 P E. The Protein Data Bank. *Nucleic Acids Res.* 2000; 28, 235-242
- 17 33. Biasini M, Bienert S, Waterhouse A, Arnold K, Studer G, Schmidt T, Kiefer F, Cassarino TG,
18 Bertoni M, Bordoli L, Schwede T. SWISS-MODEL: modelling protein tertiary and quaternary
19 structure using evolutionary information. *Nucleic Acids Res.* 2014; 42, W252-W258
- 20 34. Arnold K, Bordoli L, Kopp J, Schwede T. The SWISS-MODEL workspace: a web-based
21 environment for protein structure homology modelling. *Bioinform* 2006; 22, 195-201

- 1 1 35. Kiefer F, Arnold K, Künzli M, Bordoli L, Schwede T. The SWISS-MODEL Repository and
2 associated resources. *Nucleic Acids Res.* 2009; 37, D387-D392
3
4 2
5
6
7 3 36. Guex N, Peitsch MC, Schwede T. Automated comparative protein structure modeling with
8 SWISS-MODEL and Swiss-PdbViewer: A historical perspective. *Electrophor.* 2009; 30, S162-S173
9
10 4
11
12 5 37. Franceschini A, Szklarczyk D, Frankild S, Kuhn M, Simonovic M, Roth A, et al. STRING
13 v9.1: protein-protein interaction networks, with increased coverage and integration. *Nucleic Acids*
14 *Res.* 2013; 41, D808-815
15
16
17 7 38. Gaigalat L, Schlüter J-P, Hartmann M, Mormann S, Tauch A, Pühler A, Kalinowski J. The
18 DeoR-type transcriptional regulator SugR acts as a repressor for genes encoding the
19 phosphoenolpyruvate: sugar phosphotransferase system (PTS) in *Corynebacterium glutamicum*.
20 *BMC Mol. Biol.* 2007; 8, 104
21
22
23 9
24
25 10
26
27 11
28
29 12 39. Lee S, Sowa ME, Choi J-M, Tsai FTF. The ClpB/Hsp104 molecular chaperone—a protein
30 disaggregating machine. *J Struct. Biol.* 2004; 146, 99-105
31
32
33 13
34
35
36 14 40. Gellert M. DNA Topoisomerases. *Ann. Rev. Biochem.* 1981; 50, 879-910
37
38
39
40 15 41. Iddar A, Valverde F, Assobhei O, Serrano A, Soukri A. Widespread occurrence of non-
41 phosphorylating glyceraldehyde-3-phosphate dehydrogenase among gram-positive bacteria. *Int.*
42 *Microbiol.* 2005; 8, 251
43
44 17
45
46
47 18 42. Tomii K, Kanehisa M. A comparative analysis of ABC transporters in complete microbial
48 genomes. *Genome Res.* 1998; 8, 1048-1059
49
50 19
51
52
53 20 43. Scoccianti V, Bucchini,] AE, Iacobucci M, Ruiz KB, Biondi S. Oxidative stress and
54 antioxidant responses to increasing concentrations of trivalent chromium in the Andean crop
55 species *Chenopodium quinoa* Willd. *Ecotoxicol. Environ. Saf.* 2016; 133, 25-35
56
57
58 22
59
60 27

- 1 44. Yeh JI, Chinte U, Du S. Structure of glycerol-3-phosphate dehydrogenase, an essential
2 monotopic membrane enzyme involved in respiration and metabolism. *Proc. Natl. Acad. Sci.* 2008;
3 105, 3280-3285
- 4 45. Kim J, Chang JH, Kim EJ, Kim KJ. Crystal structure of (R)-3-hydroxybutyryl-CoA
5 dehydrogenase PhaB from *Ralstonia eutropha*. *Biochem. Biophys. Res. Com.* 2014; 443, 783-788
- 6 46. Higham DP, Sadler PJ, Scawen MD. Gold-Resistant Bacteria: Excretion of a Cystine-Rich
7 Protein by *Pseudomonas cepacia* induced by an antiarthritic drug. *J Inorg. Biochem.* 1986; 28, 253-
8 261
- 9 47. Kornberg HL, Sadler JR. The metabolism of C2-compounds in micro-organisms. VIII. A
10 dicarboxylic acid cycle as a route for the oxidation of glycollate by *Escherichia coli*. *Biochem. J.*
11 1961; 81, 503-513
- 12 48. Musrati RA, Kollárová M, Mernik N, Mikulášová D. Malate dehydrogenase: distribution,
13 function and properties. *Gen. Physiol. Biophys.* 1998; 17, 193–210.
- 14 49 Tottey S, Rondet SA, Borrelly GP, Robinson PJ, Rich PR, Robinson NJ. A copper
15 metallochaperone for photosynthesis and respiration reveals metal-specific targets, interaction with
16 an importer, and alternative sites for copper acquisition. *J. Biol Chem.* 2002; 277, 5490-5497.
- 17 50 Radford DS, Kihlken MA, Borrelly GP, Harwood CR, Le Brun NE, Cavet JS. CopZ from
18 *Bacillus subtilis* interacts in vivo with a copper exporting CPx-type ATPase CopA. *FEMS Microbiol*
19 *Lett.* 2003; 220, 105-112.
- 20 51. Pontel LB, Audero ME, Espariz M, Checa SK, Soncini FC. GoIS controls the response to
21 gold by the hierarchical induction of Salmonella-specific genes that include a CBA efflux-coding
22 operon. *Mol. Microbiol.* 2007; 66, 814-825

1 1 52. Stoyanov JV, Brown NL. The *Escherichia coli* copper-responsive copA promoter is activated
2
3
4 2 by gold. *J Biol. Chem.* 2003; 278, 1407-1410

5
6
7 3 53. Changela A, Chen K, Xue Y, Holschen J, Outten CE, O'Halloran TV, et al. Molecular basis
8
9 4 of metal-ion selectivity and zeptomolar sensitivity by CueR. *Science.* 2003; 301, 1383-1387

10
11
12
13
14
15
16
17
18
19
20
21
22
23
24
25
26
27
28
29
30
31
32
33
34
35
36
37
38
39
40
41
42
43
44
45
46
47
48
49
50
51
52
53
54
55
56
57
58
59
60

1
2
3
4
5
6
7
8
9
10
11
12
13
14
15
16
17
18
19
20
21
22
23
24
25
26
27
28
29
30
31
32
33
34
35
36
37
38
39
40
41
42
43
44
45
46
47
48
49
50
51
52
53
54
55
56
57
58
59
60
Tables

Table 1 Statistical evaluation of differently expressed spots in DIGE experiments. Minimum fold-change indicates the minimum change required to achieve a power of 80 %.

Condition 1	Condition 2	Number of differently expressed spots	q-value at significance level $\alpha = 0.05^a$	Minimum fold-change ^b
unamended	10 μ M Au(III)	684	0.0377	1.7
unamended	50 μ M Au(III)	623	0.0479	1.7
unamended	50 μ M Cu(II)	313	0.1392	1.6
10 μ M Au(III)	50 μ M Cu(II)	720	0.0396	1.6
10 μ M Au(III)	50 μ M Au(III)	169	0.3936	1.6
50 μ M Au(III)	50 μ M Cu(II)	668	0.0425	1.6

^a q-value estimates the false discovery rate in the group of all proteins detected as differentially expressed at a significance level of $\alpha = 0.05$.

^b Minimum fold-change indicates the minimum change required to achieve a power of 80 %.

Table 2 Proteins identified from DIGE gels using LC-MS. Spot numbers correspond to Fig. 1. (A) Differentially abundant proteins between both Au amended conditions and both the Cu and unamended control conditions (p-value < 0.001 and at least 3 standard deviations from the mean). (B) Spot 2087 depicts the protein spots with the highest loading in PC1 vs. PC2 for Cu-amended biological replicates. Note: only the top protein identification in terms of number of unique significant peptides and sequence coverage is reported here, for complete list see Table S3.

Spot	NCBI Accession Number version	Locus	Taxonomy	Protein description	Unique peptides ^a	Sequence Coverage [%]	pI ^b	Molecular mass [kDa]
(A)								
209	ABF09369.1	Rmet_2492	<i>C. metallidurans</i>	aconitate hydratase 1	38	62.3	6.6	97944
218	ABF08082.1	Rmet_1196	<i>C. metallidurans</i>	pyruvate decarboxylase, E1 component of the pyruvate dehydrogenase complex	33	43.8	5.8	100668
219	ABF09369.1	Rmet_2492	<i>C. metallidurans</i>	aconitate hydratase 1	28	48.7	6.6	97944
256	ABF06889.1	Rmet_0003	<i>C. metallidurans</i>	DNA gyrase, subunit B	29	48.0	5.8	93227
	ABF09369.1	Rmet_2492	<i>C. metallidurans</i>	aconitate hydratase 1	26	44.1	6.6	97944
259	ABF08838.1	Rmet_1959	<i>C. metallidurans</i>	ATP-dependent Clp protease, ATP-binding subunit ClpB (protein disaggregation chaperone)	34	52.0	5.7	95942
562	ABF07136.1	Rmet_0250	<i>C. metallidurans</i>	C-terminal processing peptidase	21	43.9	9.0	58472
586	ABF09108.1	Rmet_2229	<i>C. metallidurans</i>	ABC-type sugar transporter, periplasmic component, probable sugar binding precursor	23	52.1	8.5	64793
593	ABF09108.1	Rmet_2229	<i>C. metallidurans</i>	ABC-type sugar transporter, periplasmic component, probable sugar binding precursor	28	61.9	8.5	64793
596	ABF09108.1	Rmet_2229	<i>C. metallidurans</i>	ABC-type sugar transporter, periplasmic component, probable sugar binding precursor	29	63.6	8.5	64793
597	ABF09108.1	Rmet_2229	<i>C. metallidurans</i>	ABC-type sugar transporter, periplasmic component, probable sugar binding precursor	36	71.2	8.5	64793
600	ABF09108.1	Rmet_2229	<i>C. metallidurans</i>	ABC-type sugar transporter, periplasmic component, probable sugar binding precursor	30	67.8	8.5	64793
605	ABF09108.1	Rmet_2229	<i>C. metallidurans</i>	ABC-type sugar transporter, periplasmic component, probable sugar binding precursor	3	7.8	8.5	64793
	ABF07136.1	Rmet_0250	<i>C. metallidurans</i>	C-terminal processing peptidase	2	7.3	9.0	58472
609	ABF09118.1	Rmet_2239	<i>C. metallidurans</i>	sn-glycerol-3-phosphate dehydrogenase, aerobic, FAD/NAD(P)-binding protein	28	73.3	6.4	59059
698	ABF09118.1	Rmet_2239	<i>C. metallidurans</i>	sn-glycerol-3-phosphate dehydrogenase, aerobic, FAD/NAD(P)-binding protein	13	35.7	6.4	59059
734	ABF10537.1	Rmet_3665	<i>C. metallidurans</i>	hypothetical protein Rmet_3665 (plasmid)	19	56.5	7.7	52335
778	ABF09014.1	Rmet_2135	<i>C. metallidurans</i>	transcription termination factor Rho	17	52.4	6.8	47329
863	ABF08240.1	Rmet_1357	<i>C. metallidurans</i>	acetyl-CoA acetyltransferase (Acetoacetyl-CoA thiolase)	26	82.4	7.7	40726
874	ABF07670.1	Rmet_0784	<i>C. metallidurans</i>	phosphoribosylglycinamide synthetase phosphoribosylamine-glycine ligase	35	82.5	5.5	44714
928	ABF09801.1	Rmet_2928	<i>C. metallidurans</i>	glycolate oxidase FAD binding subunit	22	81.2	6.7	39032
977	ABF07904.1	Rmet_1018	<i>C. metallidurans</i>	tyrosine aminotransferase, tyrosine-repressible, PLP-dependent	18	64.1	6.4	43143

1060	Q1LKG0.1	Rmet_2489	<i>C. metallidurans</i>	Malate dehydrogenase	19	71.3	6.2	35163
1221	ABF07285.1	Rmet_0399	<i>C. metallidurans</i>	glutamate and aspartate transporter subunit; periplasmic-binding component of ABC superfamily	14	51.8	9.0	32940
	ABF11455.1	Rmet_4593	<i>C. metallidurans</i>	polysaccharide deacetylase (plasmid)	12	57.1	6.3	32823
	ABF08097.1	Rmet_1211	<i>C. metallidurans</i>	Putative ABC transporter, periplasmic substrate-binding protein	12	53.9	9.3	33668
	ABF09341.1	Rmet_2464	<i>C. metallidurans</i>	acetyl-CoA carboxylase, beta (carboxyltransferase) subunit	13	47.2	6.5	31764
	ABF07038.1	Rmet_0152	<i>C. metallidurans</i>	conserved hypothetical protein	11	55.8	6.3	31058
1237	ABF09114.1	Rmet_2235	<i>C. metallidurans</i>	DNA-binding transcriptional repressor	18	79.5	5.3	28476
1417	ABF06992.1	Rmet_0106	<i>C. metallidurans</i>	acetyl-CoA acetyltransferase	25	89.3	6.7	41355
1429	ABF08241.1	Rmet_1358	<i>C. metallidurans</i>	Acetoacetyl-CoA reductase	11	58.9	6.7	26360
	ABF11607.1	Rmet_4745	<i>C. metallidurans</i>	Short-chain dehydrogenase/reductase SDR (plasmid)	11	51.2	7.7	26950
	ABF10099.1	Rmet_3227	<i>C. metallidurans</i>	stringent starvation protein A	10	66.5	6.5	23787
1433								
1672	ABF09807.1	Rmet_2934	<i>C. metallidurans</i>	glutathione peroxidase	7	64.0	6.1	18414
1681	ABF07968.1	Rmet_1082	<i>C. metallidurans</i>	peptidyl-prolyl cis-trans isomerase B (rotamase B)	4	30.7	5.4	18154
1933	ABF07344.1	Rmet_0458	<i>C. metallidurans</i>	universal stress protein, UspA family	4	39.6	6.4	15091
	Q1LQS5.1	Rmet_0615	<i>C. metallidurans</i>	10 kDa chaperonin	3	49.0	5.8	10436
(B)								
2087	ABF12437.1	Rmet_5578	<i>C. metallidurans</i>	conserved hypothetical protein; putative signal peptide (plasmid)	2	17.0	8.5	9687
	ABF09813.1	Rmet_2940	<i>C. metallidurans</i>	DNA protection during starvation or oxydative stress transcription regulator protein; Metalloregulation DNA-binding stress protein	2	14.3	5.8	18047

^a number of peptides above the MASCOT homology threshold; total peptides: Ssum of significant and non-significant peptides detected by mass spectrometry, assigned by MASCOT to respective protein

^b pl: theoretical isoelectric point; ions score depicts the sum of all individual peptide ions scores relevant for the respective protein

Downloaded by UNIV OF ADELAIDE on 17/10/2011 11:09:11 AM

Table 3 Proteins identified from native 2D gel by LC-MS. Spot number corresponds to the numbers depicted in Fig. 4.

Spot	NCBI Accession Number Version	Locus	Taxonomy	Protein Description	Unique peptides ^a	Sequence coverage [%]	pI ^b	Molecular mass [kDA]
1	ABF10300.1	Rmet_3428	<i>C. metallidurans CH34</i>	conserved hypothetical protein; predicted periplasmic or secreted lipoprotein	6	26.4	9.38	29258
2	ABF08273.1	Rmet_1390	<i>C. metallidurans CH34</i>	malate synthase A	20	30.2	6.12	58841
3	ABF07098.1	Rmet_0212	<i>C. metallidurans CH34</i>	3-hydroxybutyryl-CoA dehydrogenase	7	26.8	5.87	30199
4	ABF09122.1	Rmet_2243	<i>C. metallidurans CH34</i>	conserved hypothetical protein	4	59.7	5.58	7298
5	Q1LKG0.1	Rmet_2489	<i>C. metallidurans CH34</i>	malate dehydrogenase	13	47.4	6.24	35163
5	ABF09940.1	Rmet_3068	<i>C. metallidurans CH34</i>	lipid hydro-peroxide peroxidase	8	56.6	5.83	17392
5	ABF10492.1	Rmet_3620	<i>C. metallidurans CH34</i>	multifunctional enzyme (serine-type endopeptidase / oxidoreductase) (degP / mucD-like) (plasmid)	2	6.8	6.16	50755
5A	Q1LKG0.1	Rmet_2489	<i>C. metallidurans CH34</i>	malate dehydrogenase	14	48.6	6.24	35163
5A	ABF09940.1	Rmet_3068	<i>C. metallidurans CH34</i>	lipid hydro-peroxide peroxidase	4	27.7	5.83	17392
5A	ABF10492.1	Rmet_3620	<i>C. metallidurans CH34</i>	multifunctional enzyme (serine-type endopeptidase / oxidoreductase) (degP / mucD-like) (plasmid)	2	6.8	6.16	50755
6	ABF10312.1	Rmet_3440	<i>C. metallidurans CH34</i>	conserved hypothetical protein; alkylhydroperoxidase AhpD core	4	32.9	6.72	16268
7	ABF08240.1	Rmet_1357	<i>C. metallidurans CH34</i>	acetyl-CoA acetyltransferase (Acetoacetyl-CoA thiolase)	4	10.9	7.65	40726
8	ABF11791.1	Rmet_4929	<i>C. metallidurans CH34</i>	glutathione S-transferase enzyme with thioredoxin-like domain protein (plasmid)	6	26.0	7.90	26701
8	ABF08466.1	Rmet_1583	<i>C. metallidurans CH34</i>	periplasmic L-asparaginase II	6	18.7	8.97	39691
8	ABF08240.1	Rmet_1357	<i>C. metallidurans CH34</i>	acetyl-CoA acetyltransferase (Acetoacetyl-CoA thiolase)	2	6.1	7.65	40726
9	ABF10490.1	Rmet_3618	<i>C. metallidurans CH34</i>	organic hydro-peroxide resistance protein OhrB, OsmC family (plasmid)	5	43.6	6.72	14509
10	ABF10490.1	Rmet_3618	<i>C. metallidurans CH34</i>	organic hydroperoxide resistance protein OhrB, OsmC family (plasmid)	7	45.7	6.72	14509
10	ABF09841.1	Rmet_2968	<i>C. metallidurans CH34</i>	2-Hydroxychromene-2-carboxylate isomerase	2	8.5	6.83	21809
11	ABF10490.1	Rmet_3618	<i>C. metallidurans CH34</i>	organic hydro-peroxide resistance protein OhrB, OsmC family (plasmid)	6	43.6	6.72	14509
11	ABF09499.1	Rmet_2622	<i>C. metallidurans CH34</i>	putative carboxymethylenebutenolidase (Dienelactone hydrolase)	2	7.2	7.68	31550

^a number of peptides above the MASCOT homology threshold; total peptides: Ssum of significant and non-significant peptides detected by mass spectrometry, assigned by MASCOT to respective protein

^b pI: theoretical isoelectric point; ions score depicts the sum of all individual peptide ions scores relevant for the respective protein

Table 4 Proteins identified at the position where LA-ICP-MS detected Au, shown in Fig 5B.

NCBI Accession Number Version	Locus	Taxonomy	Protein description	Unique peptides ^a	Sequence coverage [%]	pI ^b	Molecular mass [kDA]
ABF09276.1	Rmet_2399	<i>C. metallidurans</i> CH34	conserved hypothetical protein copper chaperone, heavy metal	3	34.6	5.7	11664
ABF10397.1	Rmet_3525	<i>C. metallidurans</i> CH34	ion binding (modular protein) putative Glyoxalase/bleomycin	3	27.1	8.6	14773
ABF08652.1	Rmet_1773	<i>C. metallidurans</i> CH34	resistance protein/dioxygenase 3-demethylubiquinone-9 3-	3	18.2	5.1	15767
ABF11332.1	Rmet_4467	<i>C. metallidurans</i> CH34	methyltransferase (plasmid)	2	18.8	5.1	16113
ABF09855.1	Rmet_2982	<i>C. metallidurans</i> CH34	conserved hypothetical protein	2	11.1	5.0	15693
O33522.2	Rmet_2922	<i>C. metallidurans</i> CH34	Chaperone protein DnaK	2	3.5	4.9	69786

^a number of peptides above the MASCOT homology threshold; total peptides: Ssum of significant and non-significant peptides detected by mass spectrometry, assigned by MASCOT to respective protein

^b pI: theoretical isoelectric point; ions score depicts the sum of all individual peptide ions scores relevant for the respective protein

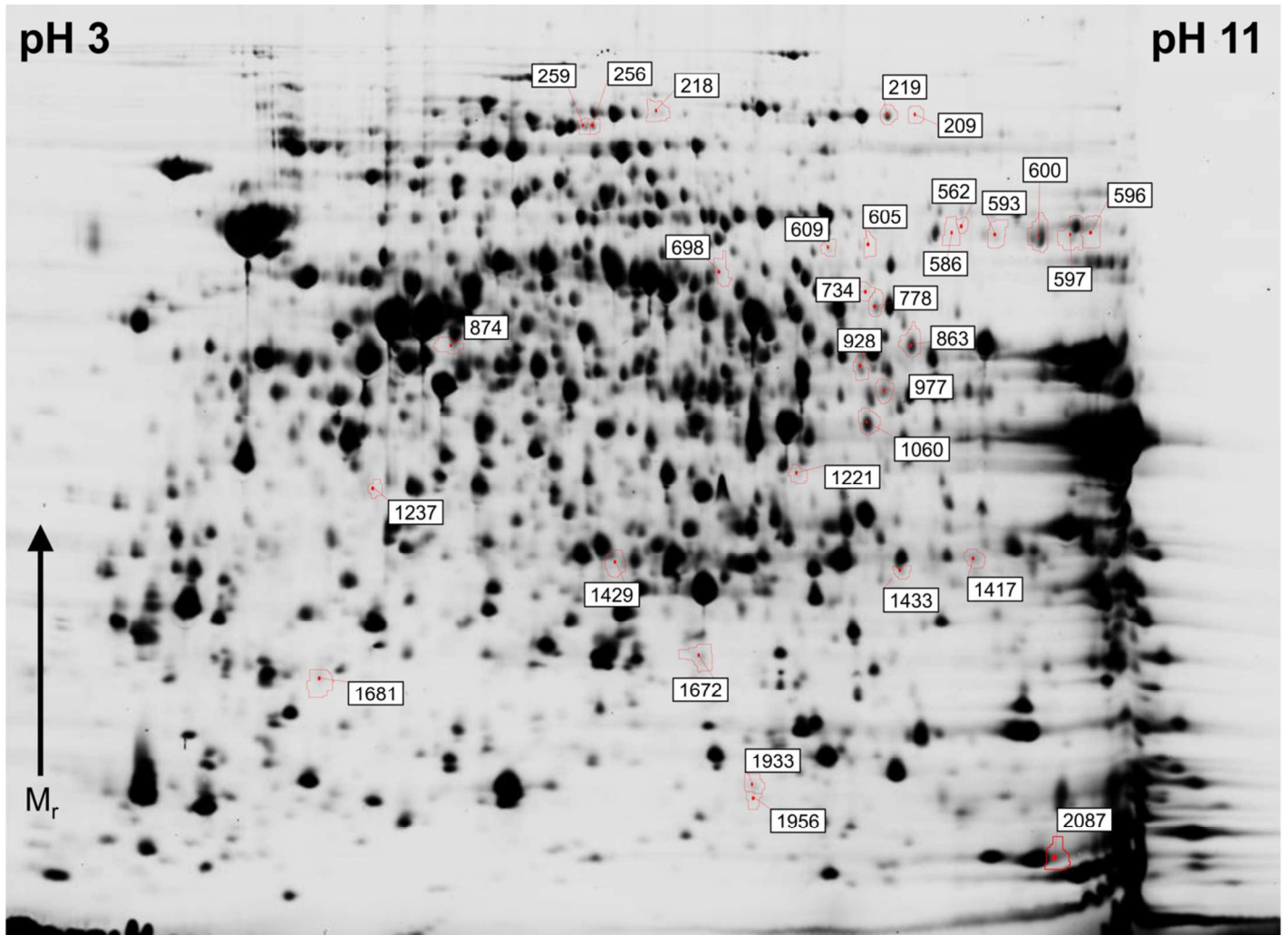
Figure Legends

- Figure 1** DIGE analysis of *C. metallidurans* CH34 grown in the presence of Au(III), Cu(II) and unamended. Representative DIGE gel, IPG 3-11NL, T=12.5%. Representative DIGE gel, numbers correspond to numbers in Table 2 and show differentially expressed proteins between *C. metallidurans* CH34 challenged with Au(III) compared to Cu(II) and the unamended cells.
- Figure 2** Principal component (PC) analysis **(A)** PC vs. PC2 and **(B)** associated biplot and **(C)** PC5 vs. PC2 and **(D)** associated biplot of DIGE protein fingerprints of the four experimental groups. *C. metallidurans* CH34 grown with Au(III) separates from other conditions in PC1 demonstrating a specific proteomic response to Au(III)-stress; PC5 vs. PC2 separates all experimental groups.
- Figure 3** **(A)** Analysis of the 152 proteins that were differentially regulated between Au(III), Cu(II) and the unamended control **(B)** Functional classification of 29 identified proteins showing the highest degree of differential expression between Au(III) and the Cu(II) / unamended controls.
- Figure 4** **(A)** Representative native 2D gel, IPG 3-10NL, 300 µg native protein extract of *C. metallidurans* grown with 50 µM Au(III)-chloride; gel was Ag-stained. Numbers depict proteins identified by mass spectrometry (see Table 3). Insert exhibits gamma-adjusted area for better visualisation of Spot 1. **(B, C, D)** detailed view of regions of interest of native 2D gels across three replicate of Cu(II), unamended and Au(III) amended cells, respectively, showing protein spots 1-11 up-regulated in Au(III) amended extracts (D).

1 **Figure 5** Results of LA-ICP-MS on native 2D Western Blot of a protein extract of *C.*
2
3
4 *metallidurans* cells challenged with 50 μ M Au(III). Shown analyses for Au, Cu and the
5
6 C background **(A)** on the corresponding native IEF dimension blot **(B)**.
7

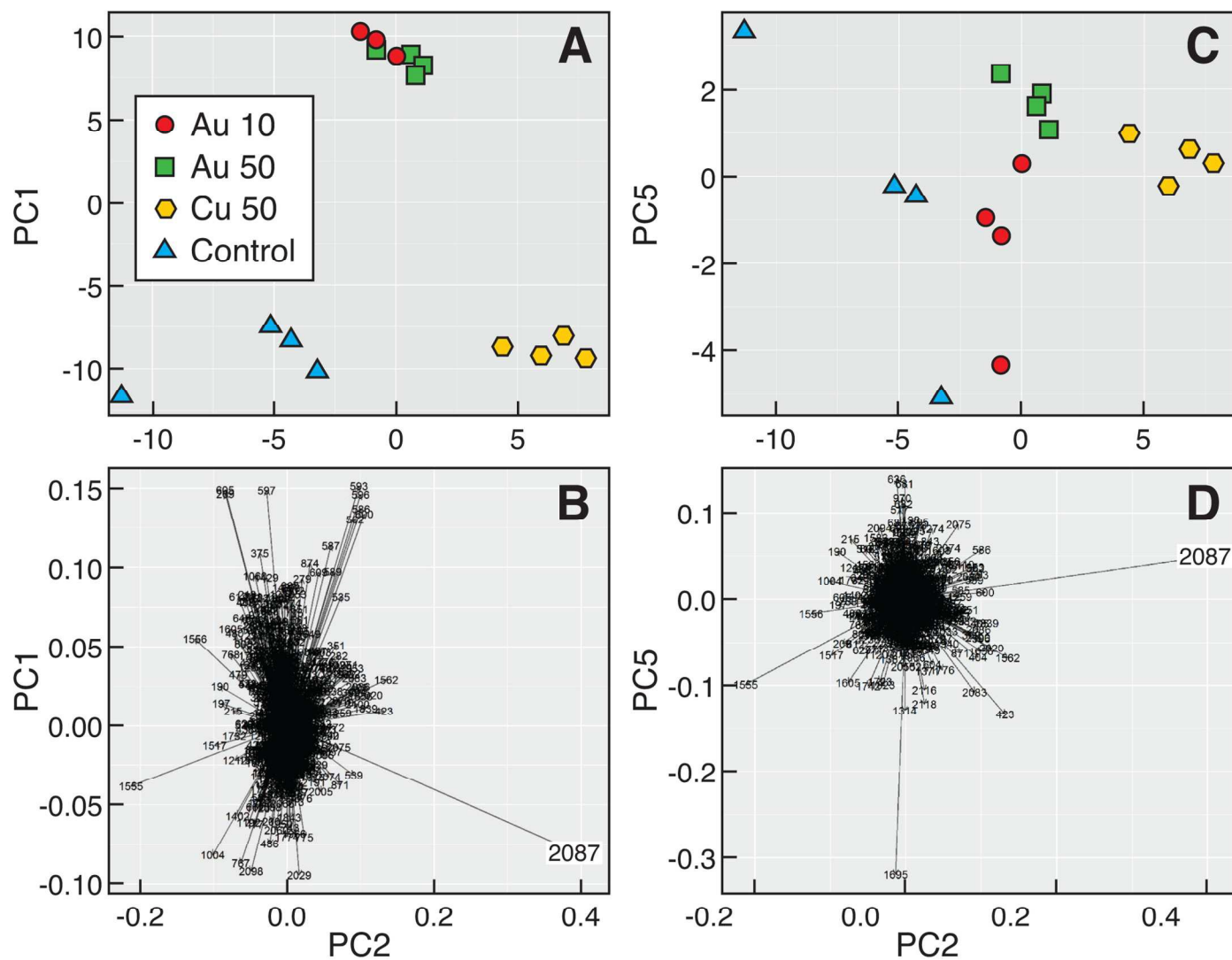
8 **Figure 6** Network visualisation of the CupC environment using STRING V.9, shown are
9
10 proteins interacting with CupC based on confidence settings of 0.9 **(A)**, indicating that
11
12 CupC may bind to a number of ATPase, including the P-type ATPase CupA, the
13
14 Pb/Cd-transporting ATPase CadA, the heavy metal transporting P-type ATPase and
15
16 the metal transporter ATPase, CtpA1, as well as the DNA-binding transcriptional
17
18 activator of copper-responsive regulon genes CupR. **(B)** Protein model of CupC from
19
20 *C. metallidurans* CH34. Protein model of CupC constructed in SWISS-PROT
21
22 modelled on CupC and two heavy metal binding proteins, *i.e.*, 2rml.1.A, a copper
23
24 transporting P-type ATPase CopC; 2rog.1.A and 2roe.1.A, both heavy metal binding
25
26 proteins (31-34) ().
27
28
29
30
31
32
33
34
35
36
37
38
39
40
41
42
43
44
45
46
47
48
49
50
51
52
53
54
55
56
57
58
59
60

Figure 1



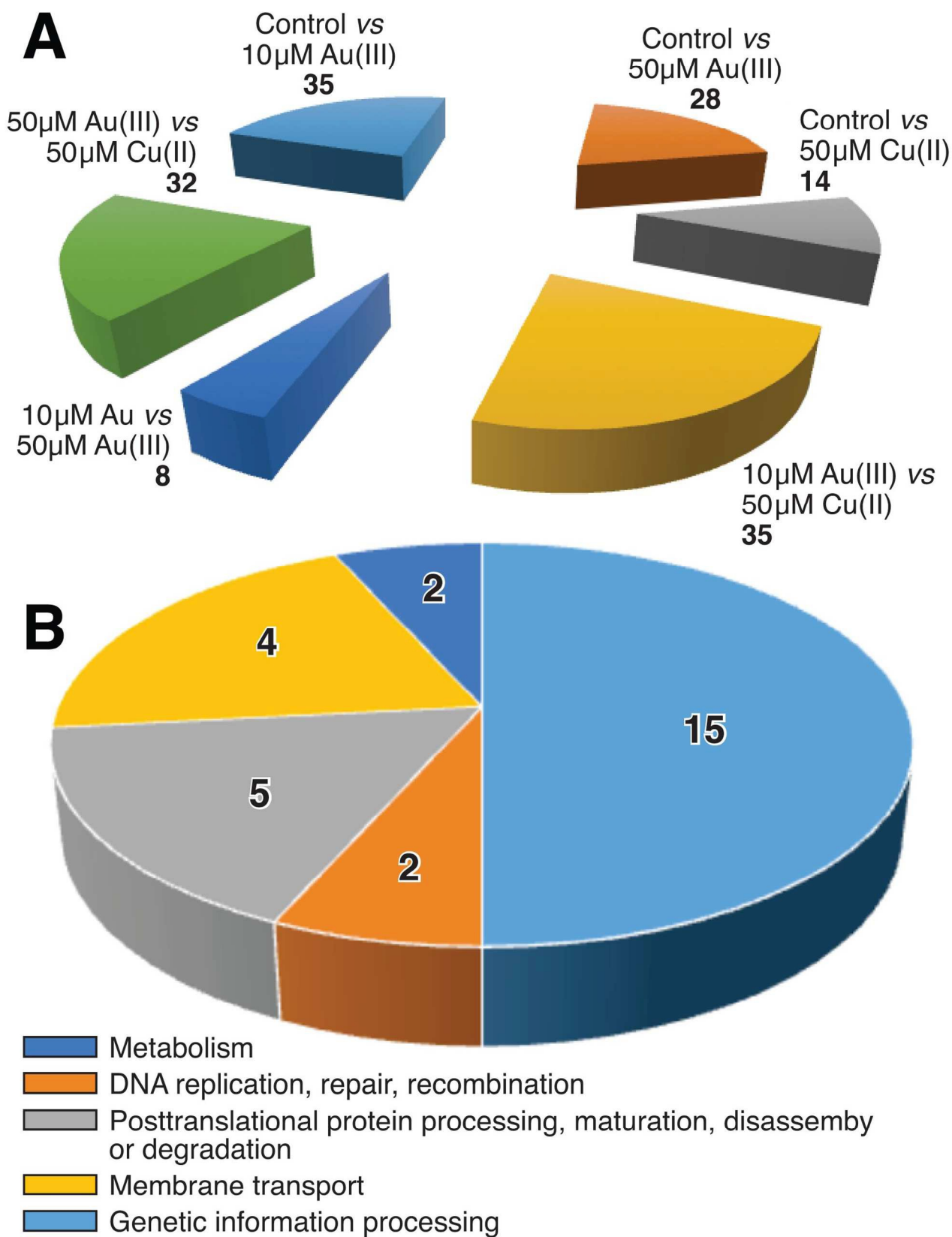
Metallomics Accepted Manuscript

Figure 2



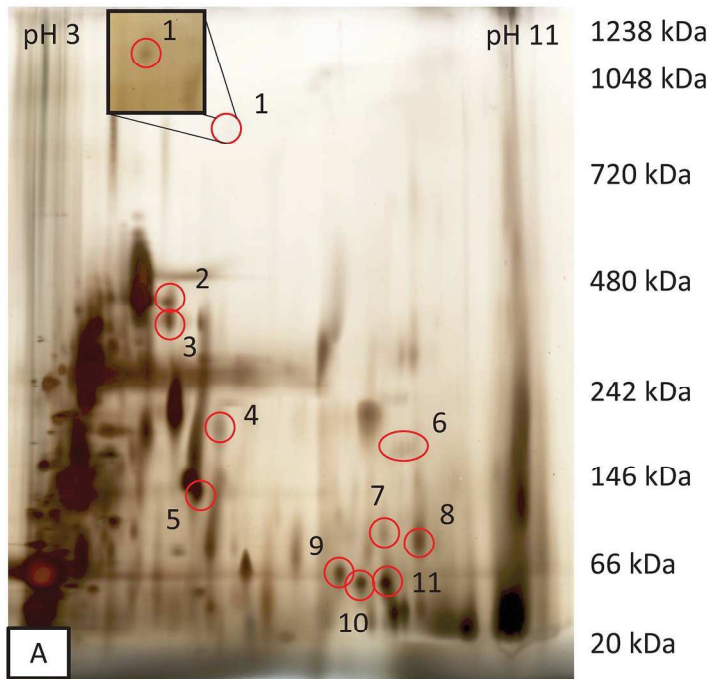
Metallomics Accepted Manuscript

Figure 3



1
2
3
4
5
6
7
8
9
10
11
12
13
14
15
16
17
18
19
20
21
22
23
24
25
26
27
28
29
30
31
32
33
34
35
36
37
38
39
40
41
42
43
44
45
46
47
48
49
50
51
52
53
54
55
56
57
58
59
60

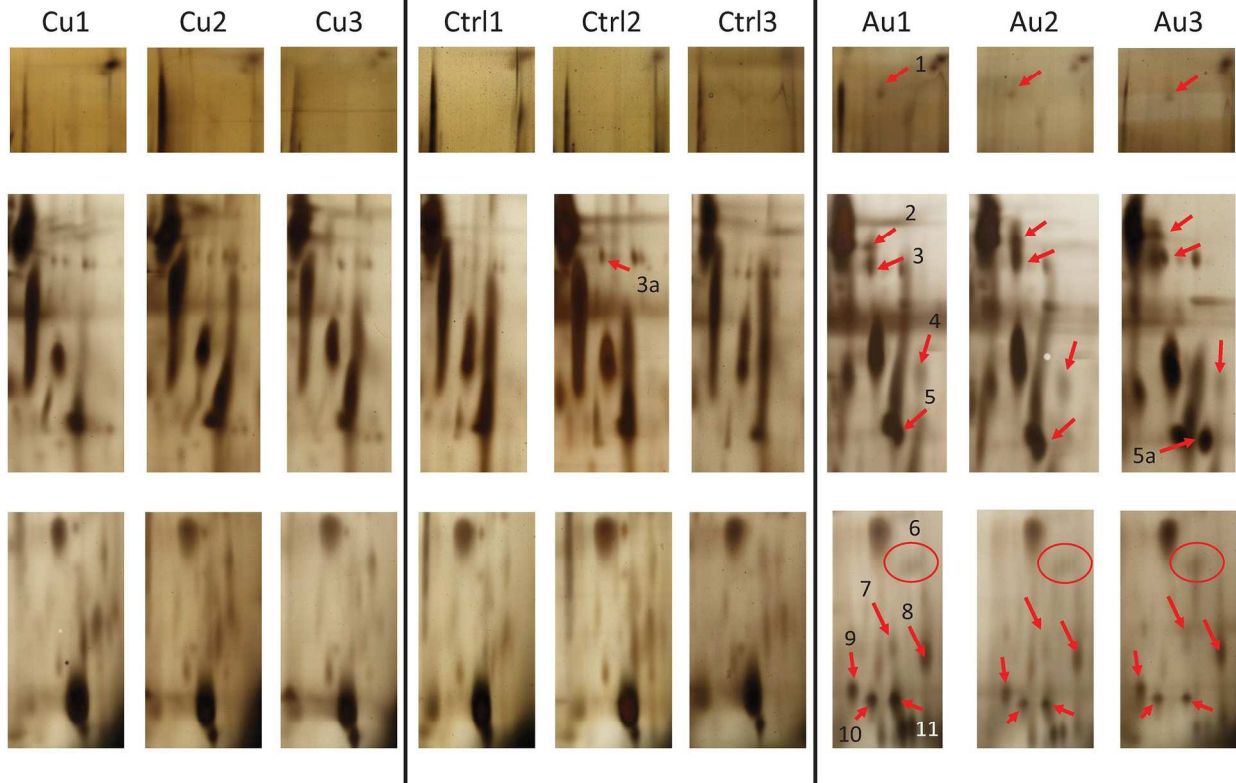
Figure 4



B

C

D



Metallomics Accepted Manuscript

Figure 5

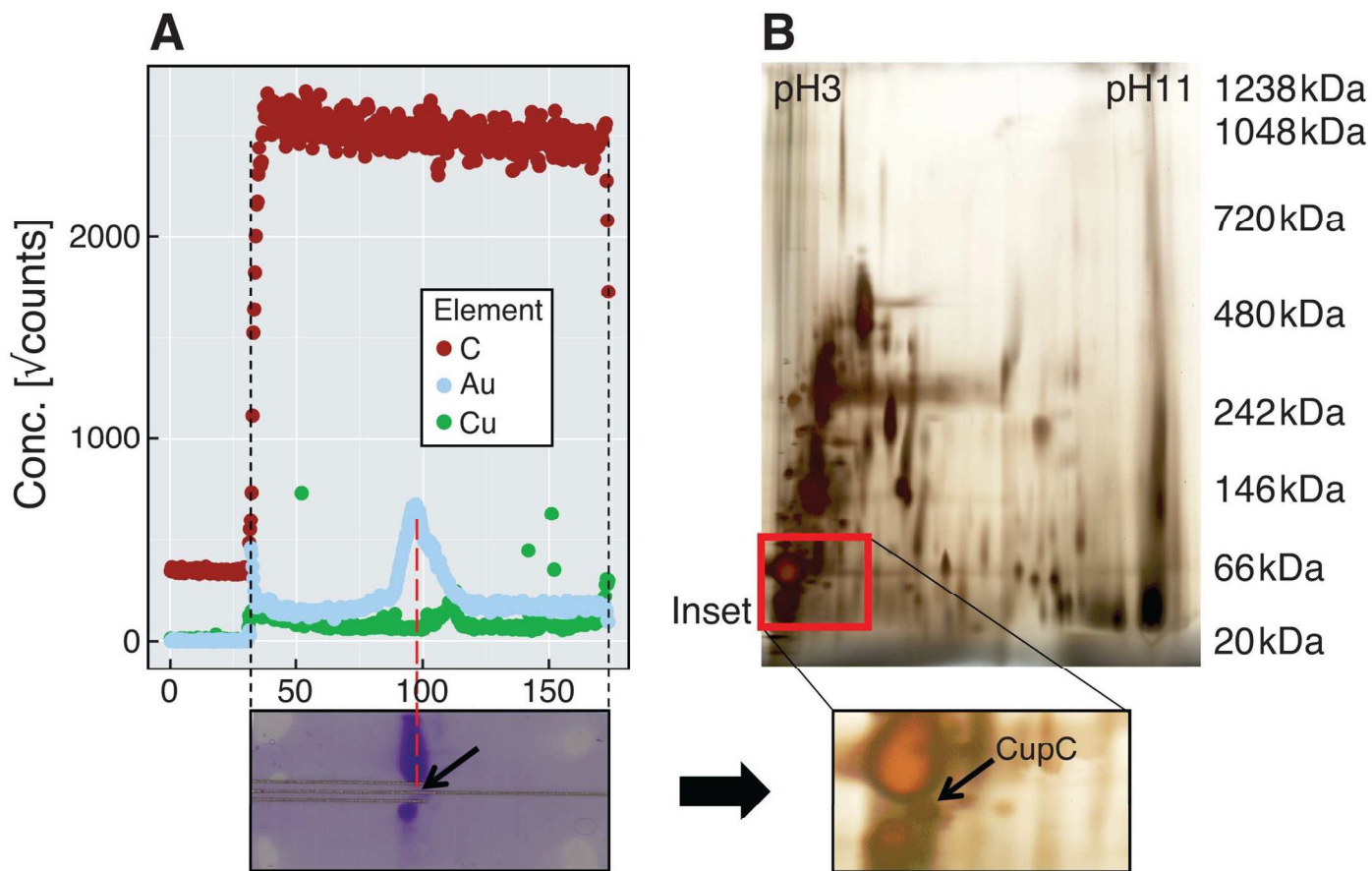


Figure 6

